

Acoustic phonon broadening mechanism in single quantum dot emission

L. Besombes* and K. Kheng

CEA-Grenoble, Département de Recherche Fondamentale sur la Matière Condensée/SP2M, 17 avenue des Martyrs,
38054 Grenoble Cedex 9, France

L. Marsal and H. Mariette

Laboratoire de Spectrométrie Physique, Université J. Fourier, Grenoble I Boîte Postale 87,
38402 Saint Martin d'Hères Cedex, France

(Received 18 July 2000; published 27 March 2001)

We study the effect of the exciton-acoustic-phonon coupling on the optical homogeneous line shape of confined zero-dimensional excitons and discuss the connection with the so-called pure dephasing effect. On increasing the temperature, the line shape progressively deviates from the expected Lorentzian profile, with the appearance of low energy acoustic-phonon sidebands. The non-Lorentzian line shape and its temperature dependence are theoretically modeled on the basis of the lattice relaxation due to the exciton-acoustic-phonon coupling. This gives a precise description of the underlying mechanism which controls the exciton dephasing.

DOI: 10.1103/PhysRevB.63.155307

PACS number(s): 78.66.Hf, 63.20.Ls, 73.61.Ga

The linewidth of an optical transition is well known to be inversely proportional to the lifetime of the radiative state. In solid crystal, with increasing temperature, *inelastic* scattering of the exciton by optical or acoustic phonons reduces the exciton lifetime and broadens the excitonic line.¹ In such a mechanism, the corresponding loss of population of the radiative state induces a loss of phase coherence (dephasing) that can be measured by four-wave-mixing experiments.

The quantum dot (QD) system was thought to be very insensitive to *inelastic* scattering by low energy acoustic phonons because of the absence of suited states between the QD discrete energy levels (bottleneck effect). However, previous studies of single QD lines have shown the persistence of some significant dephasing despite this bottleneck effect.² On the other hand, simultaneous measurements of the dephasing and the population decay for localized excitons in narrow GaAs quantum wells (QWs) show that, with increasing temperature, *elastic* interaction with acoustic phonons also contributes to dephasing.³ Such a loss of phase coherence that is not related to a population relaxation is called *pure dephasing*. Usually, pure dephasing is treated using an additional phenomenological phase damping linearly proportional to time,³ that straightforwardly leads to a Lorentzian line shape for the homogeneously broadened transition.⁴ This corresponds to assuming a so-called Markovian process for the elastic exciton-phonon interaction.⁵

In this paper, we show that this *elastic* exciton-phonon interaction in the low temperature range can no longer be described by a single dephasing rate [or a simple full width at half maximum (FWHM)] as usual.^{3,4} This is evidenced by the special temperature dependence behavior of the line shape of CdTe QD's emission: the zero-phonon line and its acoustic phonon sidebands are distinctly observed due to a suited phonon coupling strength. These two components of the emission line are well described by a theoretical model that considers recombination from stationary eigenstates formed by the mixing of the discrete excitonic states with the continuum of acoustic phonons. This allows us to give new insights into the acoustic phonon broadening mechanism

which controls the exciton dephasing and imposes the real limits to the optical properties of single QD's emission.

The observed physical effects are not specific to the quantum dots themselves, but are general to all strongly localized excitons, whatever the system. For the present study the sample consists of a nominally 6.5 monolayer CdTe structure embedded in ZnTe barriers, grown by atomic layer epitaxy. Confinement of excitons in QD's in these structures is evidenced by the observation of sharp excitonic lines by microphotoluminescence (μ -PL) spectroscopy.⁶ The single QD spectroscopy is performed through small apertures in an opaque 100 nm thick Al film deposited on the sample surface. The spatial resolution, defined by the size of the aperture, can reach 0.25 μ m. The sample is excited by the 488 nm line of an Ar⁺ laser and the PL is detected through a microscope objective. The spectral resolution of the experimental set up is about 70 μ eV.

Figure 1 shows the PL spectra of a single QD as a function of temperature and normalized to the integrated intensity. At 5 K, the emission peak presents a Lorentzian profile with 180 μ eV linewidth. With increasing temperature, the emission peak shows a redshift and a quenching of its intensity with an activation energy of about 13 meV. The main feature that we will discuss is the observed temperature dependence of the emission line shape. Surprisingly, on increasing the temperature, the PL line shape deviates from a Lorentzian: a broad background appears on both sides of the central line. We assign the central line to the excitonic zero-phonon line, and the broad background to a coupled exciton-acoustic phonon band (sidebands), as discussed later. At high temperature, the zero-phonon line disappears in the phonon sidebands. As a consequence, the FWHM of the luminescence line (Fig. 2) shows a striking behavior. It first corresponds to the linewidth of the zero-phonon line and increases slowly below 30 K. Then it includes the phonon sidebands and increases very abruptly (see inset of Fig. 2 for $T=30$ and 45 K).

We first consider the zero-phonon line. The usual lifetime broadening mechanism can account for the slow increase of

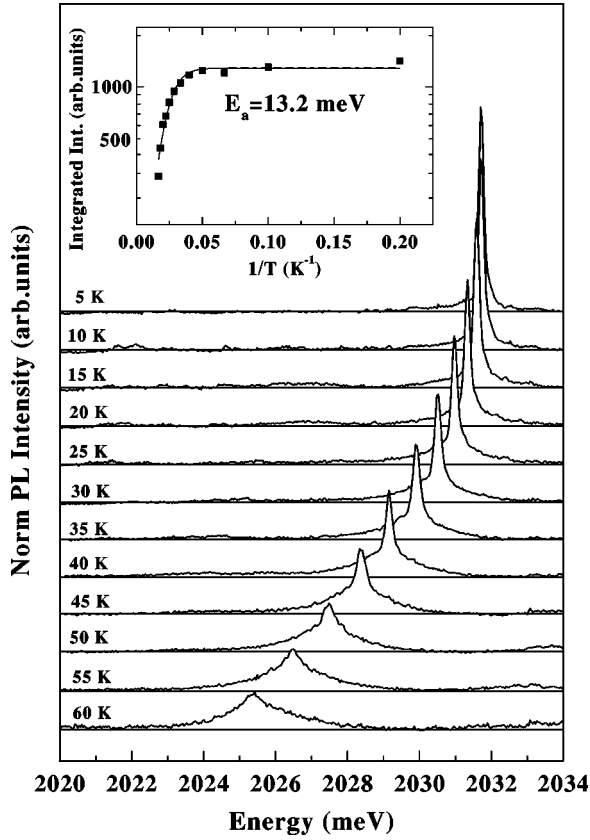


FIG. 1. PL spectra of a single QD, normalized to the integrated intensity, as a function of the temperature. With increasing T , sidebands appear progressively around the central zero-phonon line. The inset shows the evolution of the integrated intensity with temperature. The fit gives an activation energy of 13.2 meV.

the linewidth below 30 K. Both exciton radiative recombination and the phonon assisted transitions to higher energy exciton states contribute to population decay. While the radiative lifetime is nearly constant, acoustic phonon scattering increases with the temperature, broadening the transition. In 2D QW's, where a continuum of excited states is available, this broadening is linear with temperature. In a QD, due to an absence of final states with a suitable energy, the phonon induced population decay is reduced and a lower thermal broadening is expected. The thermal broadening measured in the QD ($1.5 \mu\text{eV K}^{-1}$) is indeed smaller than the one reported for a 18 \AA CdTe/Cd_{0.82}Zn_{0.18}Te QW ($3.5 \mu\text{eV K}^{-1}$).^{7,8}

Now, to describe the exciton-acoustic phonon band one must consider the mixing of the exciton with acoustic phonon modes. To do that we extend the Huang-Rhys theory of localized electron-phonon interaction¹⁰ to the exciton system in a QD. In this model, we no longer consider the exciton-phonon interaction as a perturbation, but take into account the new eigenstates resulting from the coupling of a discrete excitonic state with the continuum of acoustic phonons. Transitions from these new eigenstates give rise to the exciton-phonon band. The general Hamiltonian for a coupled exciton-phonon system is written as

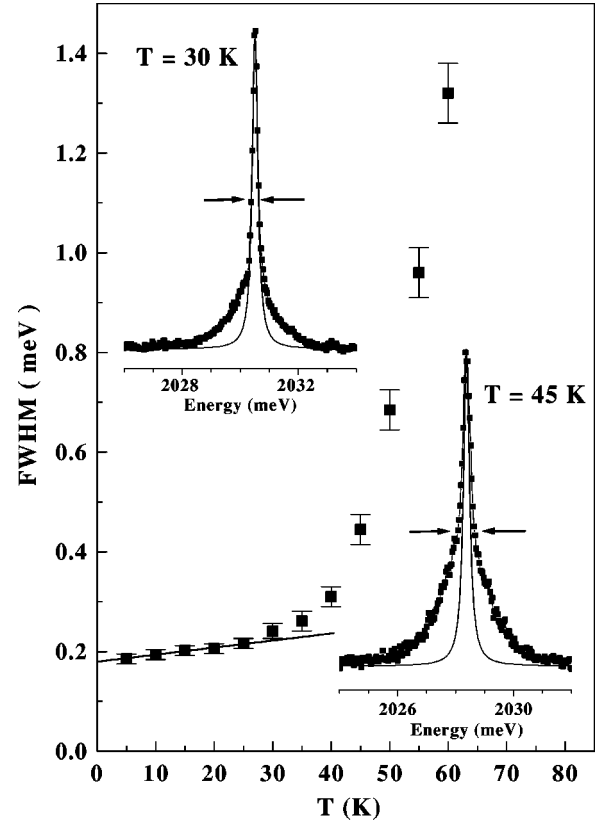


FIG. 2. Temperature dependence of the exciton PL line FWHM. The linear fit at low temperature (solid line) gives a slope of $1.5 \mu\text{eV K}^{-1}$. Insets show PL lines measured at $T = 30$ and 45 K. The line shape strongly deviates from a Lorentzian profile (solid line) and the sidebands which appear around the central zero-phonon line progressively control the FWHM.

$$H = E_0 c^\dagger c + \sum_q \hbar \omega_q^- \left(b_q^\dagger b_q^- + \frac{1}{2} \right) + c^\dagger c \sum_q M_q^- (b_q^\dagger + b_q^-), \quad (1)$$

where c^\dagger and b_q^\dagger (c and b_q^-) are the creation (annihilation) operator of the exciton (with energy E_0) and the phonon (with momentum \vec{q} and energy $\hbar \omega_q^-$), respectively. The first two terms of the Hamiltonian are the contributions of the exciton and phonon populations to the energy of the system. The last term is the exciton-phonon interaction characterized by the matrix elements M_q^- . The ground state of the system is the lattice with a phonon bath. The excited state (i.e., with the presence of the exciton), due to the exciton-phonon interaction, is no longer a pure exciton state decoupled from the phonon modes, but contains an admixture of phonon eigenstates.

In the limit where off-diagonal elements in M_q^- can be ignored, the Hamiltonian in Eq. (1) can be diagonalized analytically.¹⁰ This neglects mixing with the excited electronic states of the QD, and is valid when the thermal energy $k_B T$ is smaller than the relevant electronic level spacing. The coupling between the exciton and each phonon mode \vec{q} then changes the equilibrium lattice position and shifts the exciton energy by the temperature-independent polaron energy Δ_q^-

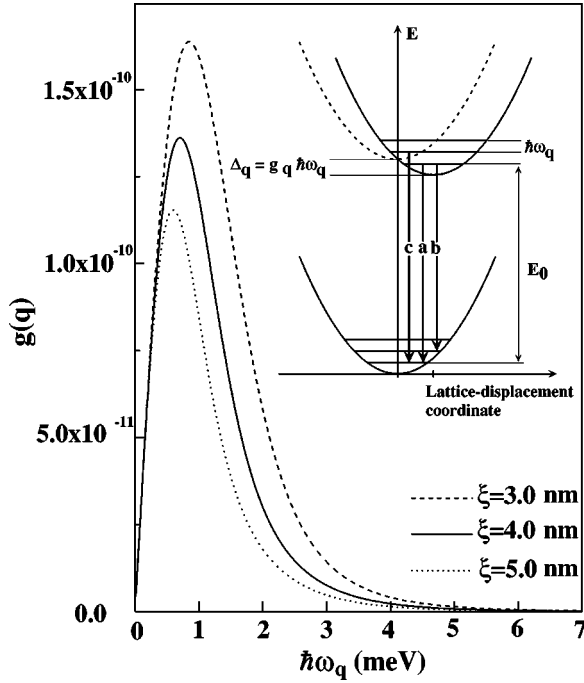


FIG. 3. Calculated coupling constant $g(q)$ as a function of the phonon energies $\hbar\omega_q = \hbar u_s q$. The inset shows the energy of the exciton-phonon system for a given phonon mode q in the configuration coordinate space. Parabolas are the harmonic potentials of the lattice in the initial and final states of the excitonic transition with (solid line) and without (dotted line) the exciton-phonon coupling. Vertical arrows labeled a, b, and c are examples of recombination processes corresponding to a zero-phonon contribution, one phonon emission and one phonon absorption, respectively.

$= M_q^2 / \hbar \omega_q = g_q^- \cdot \hbar \omega_q^-$. This equation defines g_q^- the coupling constant of the exciton with the phonon mode \vec{q} . As illustrated in the inset of Fig. 3, due to the shift of the equilibrium position when the exciton recombines, optical transitions are now allowed between states having different phonon occupation numbers, and occur with absorption or emission of phonons.

The probability that the optical transition involves p phonons is given by¹¹

$$W_p = \left(\frac{n_q^- + 1}{n_q^-} \right)^{p/2} e^{-g_q^-(2n_q^- + 1)} I_p [2g_q^- \sqrt{n_q^- (n_q^- + 1)}], \quad (2)$$

where $n_q^- = [e^{\hbar\omega_q^- / k_B T} - 1]^{-1}$ is the Bose distribution and $I_p(z)$ the imaginary argument Bessel function. Each value of p gives rise to a discrete line with height W_p on each side of the zero-phonon transition. The transition probabilities W_{p_i} of a set of N discrete phonon modes q_i with energy $\hbar\omega_{q_i}$ lead to the spectral shape function:

$$I(h\nu) = \sum_{p_1 \cdots p_N}^{\infty} W_{p_1} \cdots W_{p_N} \delta(h\nu - E_0 + p_1 \hbar\omega_{q_1} + \cdots + p_N \hbar\omega_{q_N}), \quad (3)$$

where p_i is the number of phonons in the mode q_i involved in the optical transition.

To calculate the matrix element M_q^- and transition probabilities, we make the following assumptions. (i) As shown by Takagahara,¹² the dominant interaction term between electrons and acoustic phonons arises from the deformation potential coupling to the longitudinal acoustic (LA) phonon mode. So, we neglect both the interaction with transverse-acoustic modes and the piezoelectric coupling. (ii) In self-assembled QDs, such as our CdTe/ZnTe system, the elastic properties of dot and matrix material are not much different, and thus the bulk-like acoustic-phonon modes can be used as a zero-order approximation by contrast to nanocrystal QD's.⁵ The acoustic-phonon spectrum is then taken to be the Debye spectrum $\omega(\vec{q}) = u_s q$, where u_s is the angular averaged sound velocity of the LA mode.

With these assumptions, the diagonal matrix element M_q^- for an exciton state $|X\rangle$ is given by¹²

$$M_q^- = \sqrt{\frac{\hbar |\vec{q}|}{2\rho u_s v}} (D_c \langle X | e^{i\vec{q} \cdot \vec{r}_e} | X \rangle - D_v \langle X | e^{i\vec{q} \cdot \vec{r}_h} | X \rangle), \quad (4)$$

where D_c (D_v) is the deformation potential of the conduction (valence) band, ρ the mass density, and v the quantization volume.

We consider that the confinement is stronger in the growth direction. The weaker QD lateral confinement can be considered as isotropic, since no exchange splitting is observed for the confined exciton investigated here.⁶ We choose to describe the localized state $|X\rangle$ by a quasi-two-dimensional exciton wave function with a Gaussian distribution for the center of mass motion characterized by a localization length parameter ξ .¹³ The in-plane electron-hole correlation is described by an exponential function with a single variational parameter λ_0 . This simple wave function leads to approximate analytical expressions for the matrix element (4) (see Ref. 13).

Since an isotropic dispersion relation is considered for the LA phonon mode, each mode can be characterized by its wave vector modulus q or by its energy $\hbar\omega_q$. We can then define $g(q)$, the exciton-phonon coupling constant integrated over all directions of \vec{q} . In Fig. 3, $g(q)$ is plotted for different localization lengths ξ in the extremely 2D (flat dot) case.¹³ The parameter values used in the calculation are $D_c = -5$ eV, $D_v = 1$ eV,¹⁴ $\rho = 5.51$ g cm⁻³, $u_s = 4.0 \times 10^3$ m s⁻¹,¹⁵ and $\lambda_0 = 42$ Å, which is obtained by a variational calculation.

Figure 3 shows the main characteristic of the exciton-phonon coupling: the wave vector q of phonons, which can interact significantly with the localized exciton, is limited in magnitude to about twice the inverse localization length, with the strongest coupling when $q \sim 1/\xi$. That is, phonons with energies greater than about $2 \times \hbar u_s / \xi$ (≈ 2 meV in our case) contribute very little to the exciton dephasing. This means that for large QD's (large ξ), the exciton-phonon band narrows and is masked by the width of the zero-phonon line. Moreover, the coupling constant $g(q)$ decreases when the

localization length ξ of the exciton increases. Both these effects impede observation of the exciton-phonon emission band for large QD's.

In Ref. 5, the optical linewidth in semiconductor nanocrystals was calculated using a single effective phonon mode for the confined acoustic phonons. Such an approximation is too rough to reproduce the line shape we observe. We approximate the continuum of acoustic phonons by a set of N discrete effective phonon modes q_i , each mode q_i representing a band of efficiently coupled phonons with a total coupling constant g_{q_i} . In this discrete multimode description, the integrated coupling parameter $g = \sum_i g_{q_i}$ is conserved. To get finally the spectral shape, we replace the discrete phonon peaks [δ function in Eq. (3)] by Lorentzian with the homogeneous linewidth of the zero-phonon line. This is a direct application of the Condon approximation which neglects the dependence of the exciton wave function on the configuration coordinate.

In Fig. 4, we compare the experimental PL peaks of a single QD normalized to the integrated intensity with the calculated spectra. For the calculation, $N=12$ effective modes were defined, and only 0, 1, and 2 phonon processes in the summation of Eq. (3) are necessary to account for the experimental data. A good agreement is found between experimental results and the calculated line shape for a localization length parameter $\xi=4$ nm, which corresponds to a characteristic lateral QD size of about 9 nm ($2\xi\sqrt{2\ln 2}$). Despite the large uncertainty in the parameter values used in the calculation (especially D_c and D_v), both the relative magnitude and the shape of the calculated exciton-phonon band are in good agreement with the experimental spectra. At higher temperature, namely 50 K, the difference seen between the calculated and experimental line shape can be due to two reasons. First, the optical transition involving more than two effective acoustic phonon modes should be taken into account at high temperature. Second, the off-diagonal matrix elements $M_{\vec{q}}$ are no longer negligible when the thermal energy approaches the exciton level spacing.³ Finally, let us note that in the temperature range considered (up to 60 K) scattering with optical phonons is not efficient.

To conclude, the lattice relaxation treatment of the exciton-acoustic phonon coupling accounts for the homogeneous emission line shape for single QDs: as the temperature increases, the coupled exciton-phonon state can recombine together with a change in the phonon occupation numbers,

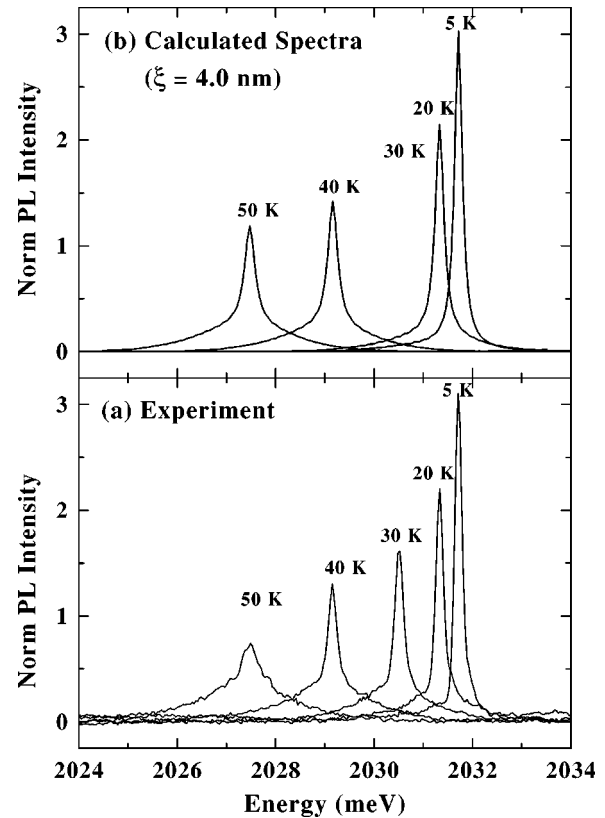


FIG. 4. (a) Experimental single exciton PL spectra, normalized to the integrated intensity, for different temperatures. (b) Calculated spectra with a localization length parameter $\xi=4$ nm. For clarity, the energy positions of the calculated spectra are set to the experimental values.

which gives rise to the exciton-phonon band surrounding the zero-phonon line. In this exciton-phonon coupling model, the pure dephasing mechanism can be viewed as a loss of phase coherence within the mixed exciton-phonon state, which is superimposed on the conventional loss of phase induced by the excitonic population decay. The characteristic temperature dependence of the emission line profile shows unambiguously that the usual description of pure dephasing by a linear phase damping breaks down for zero-dimensional excitons.

This work is part of the CEA-CNRS joint research program ‘‘Nanophysique et Semiconducteurs.’’

*Corresponding author. Electronic mail: lbesombes@cea.fr

¹D. Gammon, E. S. Snow, B. V. Shanabrook, D. S. Katzer, and D. Park, *Science* **273**, 87 (1996).

²K. Ota, N. Usami, and Y. Shiraki, *Physica E (Amsterdam)* **2**, 573 (1998).

³X. Fan, T. Takagahara, J. E. Cunningham, and H. Wang, *Solid State Commun.* **108**, 857 (1998).

⁴F. Gindele, K. Hild, W. Langbein, and U. Woggon, *Phys. Rev. B* **60**, R2157 (1999).

⁵X.-Q. Li and Y. Arakawa, *Phys. Rev. B* **60**, 1915 (1999).

⁶L. Besombes, L. Marsal, K. Kheng, T. Charvolin, L. S. Dang, A.

Wasiela, and H. Mariette, *J. Cryst. Growth* **214/215**, 742 (2000).

⁷E. J. Mayer, N. T. Pelekanos, J. Kuhl, N. Magnea, and H. Mariette, *Phys. Rev. B* **51**, 17 263 (1995).

⁸Note that the measured 5 K linewidth of the QD zero-phonon line (180 μ eV) is probably larger than the intrinsic homogeneous linewidth (Ref. 7) because of dynamical broadening processes: trapped carriers near the QD create a fluctuating electric field that slightly shifts (Stark shifts) the exciton energy (Ref. 9). The slow increase of the linewidth below 30 K reflects the lifetime decrease under the assumption that the traps, as well as the dynamical broadening, are independent of the temperature.

- ⁹J. Seufert, R. Weigand, G. Bacher, T. Kümmell, A. Forchel, K. Leonardi, and D. Hommel, *Appl. Phys. Lett.* **76**, 1872 (2000).
- ¹⁰C. B. Duke and G. D. Mahan, *Phys. Rev.* **139**, A1965 (1965).
- ¹¹G. D. Mahan, *Many-Particle Physics* (Plenum, New York, 1990).
- ¹²T. Takagahara, *Phys. Rev. B* **60**, 2638 (1999).
- ¹³T. Takagahara, *Phys. Rev. B* **31**, 6552 (1985).
- ¹⁴C. G. Van de Walle, *Phys. Rev. B* **39**, 1871 (1989).
- ¹⁵S. Rudin, T. L. Reinecke, and B. Segall, *Phys. Rev. B* **42**, 11 218 (1990).